CEAS Space Journal
https://doi.org/10.1007/s12567-023-00525-9

ORIGINAL PAPER

Assessment of radiation shielding properties of self-healing polymers and nanocomposites for a space habitat case study under GCR and LEO radiation

Laura Pernigoni[1] · **Ugo Lafont**[2] · **Antonio Mattia Grande**[1]

Received: 14 April 2023 / Revised: 25 August 2023 / Accepted: 14 September 2023

Abstract
In recent decades, the opportunity to introduce self-healing materials within space structures has drawn the attention of scientists and companies. Autonomous repair following damage caused by impacts with micrometeoroids and orbital debris (MMOD) would lead to safer human activity in space and would increase spacecraft operational life and autonomy, thus reducing replacement costs and possibly relieving astronauts from maintenance activities. In particular, integrating self-healing materials into structures to protect humans from the space environment is a fundamental step in the realization of long-lasting space exploration missions. Nevertheless, the way these materials interact with the environmental factors in space still needs to be properly analyzed and understood; in particular, space radiation is a serious threat to human health and material integrity. The proposed work hence investigates the shielding ability of candidate self-healing materials with the specific purpose of human protection in crewed missions. The NASA HZETRN2015 (High Z and Energy TRaNsport, 2015 version) software is used to simulate galactic cosmic rays (GCR) and low Earth orbit (LEO) environment. A comparison between a standard habitat layup proposed by NASA and a set of configurations containing self-healing polymers is performed to verify that the substitution of conventional bladder materials with the proposed self-healing solutions does not decrease the overall habitat shielding performance. A self-healing nanocomposite option with single-walled carbon nanotubes (SWCNTs) is also analyzed to determine whether the insertion of nanofillers can increase the overall shielding performance. In the second phase, the comparison of puncture tests on blank and irradiated samples under conditions reproducing a space suit example is presented to assess the possible effects of radiation on the self-healing performance.

Keywords Self-healing · Space radiation · Radiation shielding · Nanocomposites

Abbreviations

CME	Coronal mass ejections
DBTDL	Dibutyltin dilaurate
DGEBA	Diglycidyl ether of bisphenol A
EMU	Extravehicular Mobility Unit
GCR	Galactic cosmic rays
HZETRN2015	High Z and Energy TRaNsport, 2015 version
ICRU	International Commission on Radiation Units & Measurements
IPDI	Isophorone diisocyanate
LEO	Low Earth orbit
MI	Methylimidazole
MLI	Multilayer insulation
MMOD	Micrometeoroids and Orbital Debris
PPG	Poly(propylene glycol)
PUU	Poly(urea) urethane
SPE	Solar particle event
SWCNT	Single-walled carbon nanotubes
UDETA	2-Aminoethyl-imidazolidone
UV	Ultraviolet
Q	ICRP-60 quality factor (-)
S_j	Stopping power of a charged particle j (keV/μm)

✉ Laura Pernigoni
laura.pernigoni@polimi.it

Ugo Lafont
ugo.lafont@esa.int

Antonio Mattia Grande
antoniomattia.grande@polimi.it

[1] Department of Aerospace Science and Technology, Politecnico Di Milano, Via La Masa 34, 20156 Milan, Italy

[2] European Space Research and Technology Centre, European Space Agency, Keplerlaan 1, PO Box 299, 2200 AG Noordwijk, The Netherlands

Published online: 14 October 2023

Δt_{exp}	Equivalent exposure time (years)
φ	Solar modulation parameter (MV)

1 Introduction

Flexible and inflatable structures are being considered for future space exploration as they are lightweight and have high packing efficiency [1] that can reduce storage, transport, and associated launch costs. Nevertheless, they have low mechanical properties, and their structural integrity in space would be threatened by impacts with micrometeoroids and orbital debris (MMOD) which could lead to punctures and subsequent depressurization. This would result in mission failure and would likely be fatal to astronauts in the case of a crewed mission [2]. A solution to this issue is represented by self-healing polymers, which have become appealing for the space sector in the last two decades as they could lead to fast and autonomous repair and increase the lifetime and safety of future spacecraft while keeping them reasonably lightweight.

Nevertheless, it must be verified that the replacement of standard materials with self-healing polymers does not lead to a decrease in the radiation shielding performance of a multilayer space system. Radiation is in fact known to have detrimental effects both on material performance and human health and must hence be shielded as much as possible. The Sun and galactic cosmic rays (GCR) are the main sources of radiation in space, but trapped particles may also become relevant when a spacecraft is close to the Earth's Van Allen belts [3].

The Sun emits all wavelengths in the electromagnetic spectrum, but its main components are visible, infrared, and ultraviolet (UV) radiation. Episodic explosions called solar flares and coronal mass ejections (CME) also take place on its surface, releasing highly energetic X-rays, gamma rays, and fluxes of charged particles (protons and electrons) called solar particle events (SPE). It is not possible to exactly determine the time of occurrence of CME and SPE, but it is known that up to 3 events can sometimes happen in a single day during a solar maximum [4]. On the other hand, GCR, probably originated from the explosion of distant supernovas, permeates interplanetary space and consists of heavy, positive ions moving at velocities close to the speed of light [5]. More precisely, it is formed by approximately 85% hydrogen (protons), 14% helium, and 1% high-energy and highly charged ions called HZE particles [6]. These particles are affected by the Sun's magnetic field: their intensity is maximum during minimum solar activity, and vice versa. GCR, SPE, and radiation belts are extremely dangerous for both materials and living organisms as they are highly penetrating [7].

The here-presented research considers both the shielding ability and the possible changes in damage restoration performance of a set of self-healing materials candidate for space applications. The first part focuses on the fundamental aspect of human radiation protection during crewed missions and aims at verifying that the proposed self-healing options can be used as valid substitutes for commonly used solutions in space structures without decreasing the related overall shielding performance. For this purpose, a numerical analysis is carried out through simulation of GCR and low Earth orbit (LEO) radiation with the NASA HZETRN2015 software, focusing on the case study of an inflatable space habitat. A configuration equipped with a standard bladder [8] is compared with solutions containing self-healing polymers. The analyzed results are expressed through dose equivalent versus the layup depth, and the ultimate relevant information is given by the overall dose absorbed by tissue when shielded by the complete multilayer habitat configuration. Neat self-healing polymers are considered and used to replace the standard bladder materials, and their shielding properties are compared. The insertion of carbon nanotubes into one of the studied materials is subsequently considered to assess if nanofillers can lead to any improvements in the radiation shielding performance.

The second part of this article briefly introduces the case study of an Extravehicular Mobility Unit (EMU) space suit and compares the results of puncture tests on blank and irradiated self-healing samples, to assess possible effects of radiation on the self-healing performance of the presented materials.

2 Materials and methods

This work initially analyses the shielding performance against GCR and trapped particles radiation sources of self-healing materials, candidate as components of an inflatable space habitat, through numerical simulations carried out with the HZETRN2015 software. As described in subsect. 2.2, two examples of radiation scenarios are investigated. It is important to remember that elements with low atomic number block primary particles and generate a small number of secondary particles [9]. For this reason, it is expected that the materials with higher hydrogen content will give better shielding, as opposed to materials characterized by molecules composed of heavy atoms. This will be verified through the results from simulations.

In the second phase, preliminary irradiation tests on the considered self-healing polymers and the related puncture test device and parameters are also introduced and described focusing on the example of an EMU suit.

The choice of the habitat and EMU examples for the radiation simulations and the puncture tests respectively is

dictated by the fact that the radiation aspect is more challenging in the first case (longer exposure times), while the risk of puncture becomes more critical for the space suits (stronger thickness requirements lead to more stringent limitations to the number and extension of the involved impact protection layers).

2.1 Materials

This subsection lists the self-healing polymers analyzed both in terms of radiation shielding and self-healing performance after puncture, along with their main properties.

Reverlink® HR: Reverlink® HR (Arkema) is a supramolecular polymer with epoxy-based networks. Its density is around 1.09 g/cm^3, and it has a glass transition temperature between 5 °C and 15 °C [10]. Reverlink® HR contains both chemical and supramolecular hydrogen-bonded crosslinks and is obtained with a two-step synthesis process [11, 12]. In the first step, the Pripol 1040 fatty acid mixture reacts with 2-aminoethyl-imidazolidone (UDETA), using a [NH_2]/[COOH] molar ratio equal to 0.5, and a waste of H_2O is produced in the [NH_2]/[H_2O] ratio equal to 1. In the second phase, the remaining -COOH groups react with a bifunctional epoxide, diglycidyl ether of bisphenol A (DGEBA), in the presence of 2-Methylimidazole (2-MI) catalyst. The amount of DGEBA is adjusted to have equal molar concentrations of carboxylic acids and epoxy: [COOH] = [DGEBA]. For the sake of clarity, this polymer will be simply indicated as supramolecular elastomer in the remaining part of the paper.

Poly(urea) urethane: This urethane is obtained from trifunctional isocyanate-terminated pre-polymer PU 6000, organized into networks connected by aromatic disulphide linkages and containing urea-related H-bonds [13]. PU 6000 can be synthesized through the interaction of poly(propylene glycol) (PPG) and isophorone diisocyanate (IPDI) in the presence of the dibutyltin dilaurate (DBTDL) catalyst [14]. It will be referred to as a self-healing PUU elastomer in the paper.

The self-healing properties characterizing these two polymers originate from different mechanisms: Reverlink® HR is based on dynamic hydrogen bonds, while the PUU elastomer contains dynamic covalent bonds.

In the phase dedicated to radiation simulations, these polymers are compared to a standard bladder as part of an inflatable multilayer space habitat represented by the slightly modified example presented in [8]. Table 1 shows the inputs required for each of the considered materials by the HZETRN software, represented by density, type, and number density (atoms per unit mass) of the contained atomic species.

A self-healing nanocomposite case is also studied in which single-walled carbon nanotubes (SWCNT) are added to Reverlink® HR to understand the effect of nanofillers on the radiation shielding performance. As a matter of fact, considering that materials with lighter nuclei particles (lower atomic mass) are expected to have a better shielding behavior [15], and despite carbon not being as light as hydrogen, SWCNTs might in some cases increase the shielding performance of the material to which they are added.

2.2 Numerical simulations

The used reference space habitat multilayer configuration (Table 2) is a slight modification of the example presented by NASA in [8], with the only difference of having a bladder made from urethane-coated nylon rather than Cadpak® HD200. This choice is dictated by the lack of information on the composition of Cadpak®, which is indispensable for the simulations. The authors hence switched to standard space suit bladder materials [8], keeping the thickness used in the suit. This assumption is deemed acceptable for the here-presented preliminary analysis. Additional habitat materials information is provided in Appendix A.

The benchmark habitat is initially compared to two configurations in which the common redundant bladder (layers 14 and 16) is replaced by the supramolecular elastomer and the self-healing PUU, respectively. The purpose is to verify that the self-healing solutions can be used to replace conventional bladder materials and hence provide autonomous damage recovery to the proposed habitat without decreasing the shielding performance of this structure, which would result in higher radiation risks for the astronauts. In the second phase, a habitat layup containing a self-healing nanocomposite bladder is also studied and compared to the reference and neat configurations. The aim is to determine if and to what extent the addition of nanofillers can increase the overall shielding performance. The supramolecular elastomer is selected as the matrix, and the 1% and 10% SWCNT weight percentages are analyzed, remaining below the 20% threshold imposed by practical limitations in the composite processing [16].

Table 1 Number densities and material densities

Material	Atoms/g					Density (g/cm^3)
	H	C	N	O	S	
Supramolecular elastomer	6.10e22	3.69e22	2.05e22	1.04e22	-	1.090
Self-healing PUU	4.46e22	3.08e22	4.62e21	4.62e21	1.54e21	1.000

Table 2 Standard space habitat layers [8]

Layer	Thickness (cm)	Name	Materials	Thickness (g/cm^2)
1	0.0231	Deployment system	Kevlar®	0.0332
2	0.0048	Passive thermal MLI	Kapton®	0.00684
3	0.0489	Passive thermal MLI	Mylar®	0.0684
4	0.0048	Passive thermal MLI	Kapton®	0.00684
5	0.0302	MMOD bumper out	Nextel™	0.08154
6	1.6929	MMOD spacer	Polyurethane foam	0.02441
7	0.0302	MMOD bumper mid	Nextel™	0.08154
8	1.6929	MMOD spacer	Polyurethane foam	0.02441
9	0.0302	MMOD bumper rear	Nextel™	0.08154
10	1.6929	MMOD spacer	Polyurethane foam	0.02441
11	0.1390	MMOD rear wall	Kevlar®	0.20016
12	0.1786	Woven restraint layer	Vectran® webbing-woven	0.24998
13	0.0137	Kevlar® felt	Kevlar®	0.01968
14	0.028	Bladder	Nylon	0.0078
			Urethane	0.022
15	0.0137	Kevlar® felt	Kevlar®	0.01968
16	0.028	Bladder	Nylon	0.0078
			Urethane	0.022
17	0.0137	Kevlar® felt	Kevlar®	0.01968
18	0.0173	Inner liner	Nomex®	0.02392

*From outermost (1) to innermost (18). (14,16) = redundant bladder layers

The NASA HZETRN2015 open-source software tool [17] is chosen to simulate the irradiation of the analyzed materials. This version is preferred to the latest one (2020) as it features the slab execution mode, considered more convenient than the 3D mode available in both versions since it is less complex but satisfactory for a preliminary study. In the slab mode, the different habitat configurations (benchmark and self-healing) are modeled as multilayer geometries in which each material layer is treated as a slab and the setup has normally incident environment boundary conditions.

The focus is set on dose equivalents absorbed by human tissue when shielded by the habitat. The tissue model proposed by the International Commission on Radiation Units & Measurements (ICRU) [18] is used and assumed to be immediately behind the multilayer. The internal habitat atmosphere is hence not considered in the simulations; this is believed to be acceptable for an initial analysis.

Solar minimum conditions (maximum GCR intensity and low probability of SPE occurrence) are considered in the first set of simulations. HZETRN relies on the Badhwar-O'Neill model described in [19] to generate the spectra of the ions related to GCR. Inputs can be mission dates or a solar modulation parameter φ in units of MV. This second option is chosen for the here presented simulations, setting φ = 400 MV (solar minimum).

A LEO mission scenario is also analyzed to study the response to trapped proton and neutron albedo, referring to a database available in HZETRN2015 and covering the period from 1965 to 2015. This database contains trapped proton spectra generated through Badavi's model [20] for a circular orbit at an altitude of 400 km and an inclination of 51.6°. GCR and trapped proton and neutron albedo historical mission data from the year 1965 are here considered as an example.

The resulting total absorbed equivalent doses are compared. To evaluate radiation's stochastic effects on the human body (e.g. cancer mortality and genetic damage), as already stated the equivalent dose is the chosen output of the simulations. The ICRP-60 quality factor Q, expressed as a function of the stopping power S_j of a charged particle j (Eq. 1) [21]:

$$Q = \begin{cases} 1 & 0 < S_j \leq 10\ \text{KeV}/\mu m \\ 0.32S_j - 2.2 & 10 < S_j \leq 100\ \text{KeV}/\mu m \\ \frac{300}{\sqrt{S_j}} & S_j > 100\ \text{KeV}/\mu m \end{cases} \quad (1)$$

is selected to convert the absorbed doses in Gy into equivalent doses in Sv. Their amount per day versus the depth of the materials' layers is analyzed, as lower doses absorbed at a certain thickness correspond to higher shielding performance [21]. Thicknesses are indeed indicated in g/cm^2 (cumulative areal density), as typically done in radiation analysis. In the case under study, this does not introduce relevant inaccuracies or discrepancies in the results when moving from areal thickness to proper thickness in cm, as the

densities of the materials considered in the bladder (standard materials, supramolecular elastomer, and self-healing PUU) are all comparable and close to 1 g/cm^3.

2.3 Irradiation tests: samples manufacturing and experimental setup

All the material samples used in irradiation and puncture tests (Fig. 1) have a nominal diameter of 20 mm. The PUU specimens have a thickness of 1 mm, whereas the supramolecular elastomer ones have thicknesses ranging from 1.5 to 2 mm, due to difficulties in the manufacturing of samples with homogeneous thickness.

Part of the samples are exposed to 100 Gy radiation doses emitted at 11.1 Gy/min rate by a Cobalt-60 source placed at a distance of 60.96 cm from the target. No intermediate step is considered during irradiation, focusing on the effects of the overall target dose only. The irradiation process is performed in air, and the samples are subsequently stored in a cold room until the time of puncture tests to preserve chemical bond deterioration generated by exposure to gamma rays.

2.4 Puncture tests

Before proceeding with the puncture tests, related to the EMU suit example, humidity is removed from the blank and irradiated samples through a 24-h drying cycle. The samples are subsequently inserted between two polyamide films and fixed to the cylindrical pressure vessel of the experimental device used for evaluation of their self-healing performance (Fig. 2).

The system is then pressurized to a relative pressure of 30 kPa with an ensured continuous air supply to reproduce the reference conditions inside the EMU space suit. A vertically actuated puncheon is set into motion by the MTS 858 Mini Bionix® II machine (Fig. 3) and used to puncture the samples at a speed of 8.467 mm/s, in accordance with the ASTM F1342/F1342M-05 reference standard. During the tests, a dedicated flow meter measures the puncture-generated leakage flow rate. Each specimen is tested three times, trying to puncture the supramolecular samples in regions with similar thicknesses, around 1.5 mm. Maximum and minimum flow rates, the time between them, and the air volume lost within the 3 min right after puncture are considered as self-healing performance parameters. The main idea behind these tests is that finding a zero flow rate at a given

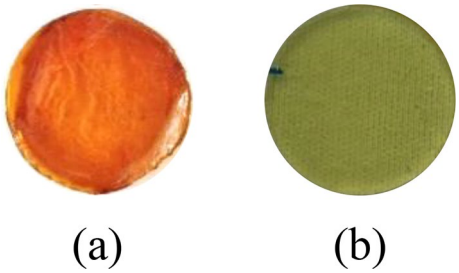

Fig. 1 Samples—**a** Supramolecular elastomer, **b** PUU

Fig. 3 MTS 858 Mini Bionix® II machine for puncture tests

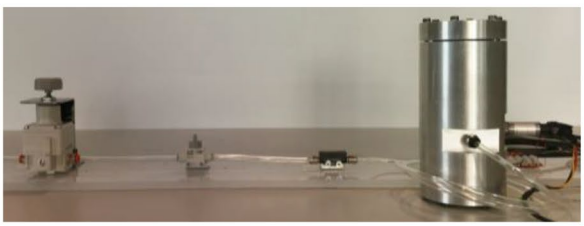

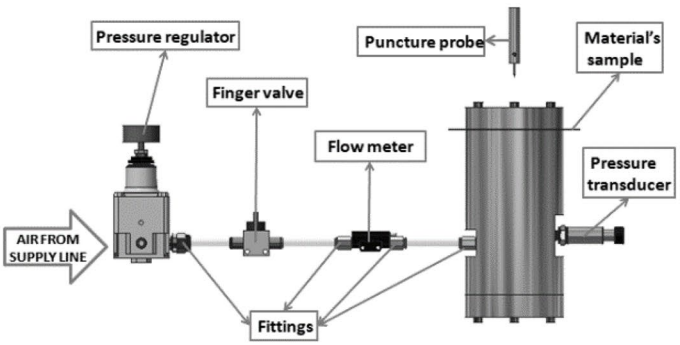

Fig. 2 Testing system

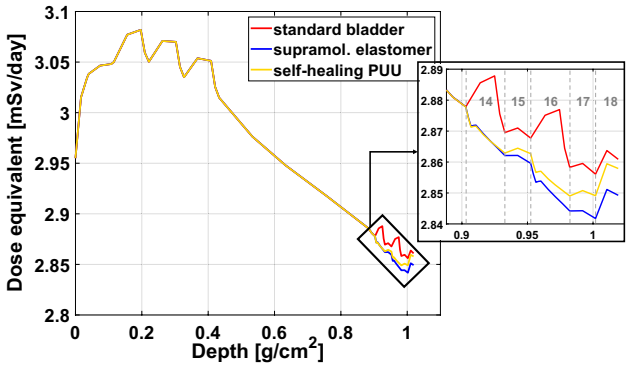

Fig. 4 Total GCR equivalent doses. The numbers in the zoomed area indicate the layers (14,16: bladder)

time would correspond to effective and complete autonomous healing of the sample under analysis.

3 Results and discussion

3.1 Numerical simulations

The results obtained from the comparison of the different habitat configurations under GCR are shown in Fig. 4. As expected, the curves remain identical up to layer 14, since the materials used in the layups are the same except for the ones chosen for the bladders. It is important to underline that the relevant dose value to be considered is the one related to the 1.01921 g/cm^2 overall areal thickness of the habitat, as it is the actual dose absorbed by tissue shielded by the whole habitat.

The plots demonstrate that the replacement of standard bladder materials with the proposed self-healing polymers does not decrease the GCR shielding performance, as they in fact introduce a slight improvement in these terms. The best option is represented by the supramolecular elastomer configuration, followed by the PUU setup. This result is consistent with the fact that Reverlink® HR is the polymer with the highest hydrogen content, and it is hence reasonable to have slightly better radiation protection in the related configuration.

As concerns the irradiation simulations in LEO, the supramolecular elastomer bladder once again leads to a slightly higher shielding performance, with a stronger improvement than in the GCR case (1.8% absorbed dose decrease with respect to the standard configuration, against the 0.4% decrease in the GCR case, Table 3).

In general, an objection that could be raised is that at a fixed density thickness the equivalent thickness in cm is higher for materials with lower density, hence the total equivalent dose in mSv/day is larger (the curve shifts rightwards) [21]. However, since the densities of the standard bladder and self-healing materials are close, the dose-versus-density depth curves can be directly used to compare them.

Table 3 Overall dose equivalents absorbed by tissue in the different configurations

Bladder type	Overall equivalent dose (mSv/day)		Δdose%	
	GCR	LEO	GCR	LEO
Standard	2.861	1.227	–	–
Supramolecular elastomer	2.849	1.205	0.4%	1.8%
Self-healing PUU	2.858	1.225	0.1%	0.2%

Table 3 shows the ultimate absorbed doses and the percentage dose reduction introduced by the self-healing solutions with respect to the standard bladder configuration (Eq. 2):

$$\Delta dose\% = \frac{standard\ dose - SH\ dose}{standard\ dose} \times 100 \tag{2}$$

Even if the improvement in shielding is almost irrelevant in the simulated GCR and LEO conditions, the results prove that replacing the standard bladder with a self-healing equivalent can provide the habitat with the additional ability to autonomously repair without decreasing its radiation protection performance.

When comparing the neat and nanocomposite supramolecular solutions, on the other hand, it is noticed that nanofillers do not lead to any relevant improvement in the radiation shielding performance of the polymer, and they indeed even introduce a slight deterioration in these terms. As a matter of fact, the GCR dose remains more or less the same when moving from the neat to the 1% SWCNT configuration and slightly increases from 2.849 to 2.85 mSv/day in the 10% SWCNT case. Under LEO conditions, a mild increase is also recorded from 1.205 mSv/day in the neat supramolecular elastomer to 1.206 mSv/day and 1.208 mSv/day in the 1% and 10% SWCNT configurations respectively. For the case under study, due to the complexity, manufacturing challenges, and high cost of the nanofillers, the nanocomposite option does not introduce any advantage and should hence be discarded in favor of neat configurations, which are much more affordable and easier to manufacture.

3.2 Puncture tests

A comparison of the results for irradiated and blank PUU samples (Fig. 5a) shows an apparent deterioration of the healing performance under the experimental dose of 100 Gy. This is clear from the average minimum flow rate and leakage time values shown in Table 4, which increase in one

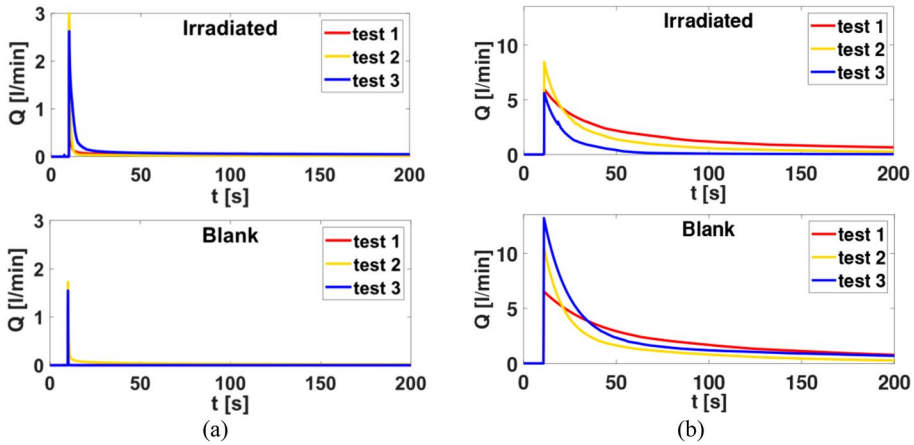

Fig. 5 Irradiated and blank samples puncture tests comparison: **a** self-healing PUU; **b** supramolecular elastomer

Table 4 Puncture test results for blank and irradiated samples, average values

Material		Q_{max} (l/min)	Q_{min} (l/min)	Δt (s)	V_{leak} (l)
Supramol. elastomer	Blank	10.11	0.57	189	5.69
	Irradiated	6.67	0.31	189	3.21
Self-healing PUU	Blank	1.51	0.005	67	0.04
	Irradiated	2.82	0.03	189	0.18

order of magnitude after irradiation. On the other hand, the effects on the supramolecular polymer seem to be milder and in contrast with the ones on PUU (Fig. 5b), as the average parameters are slightly lower for the irradiated samples. Nevertheless, this outcome for the supramolecular elastomer might actually be a consequence of the high sensitivity of this material to humidity, related to the different times at which the tests were performed, and to variability in the sample thicknesses, as it was more difficult to obtain homogeneous dimensions than in the PUU case.

It can be seen that for the considered 100 Gy radiation dose the here-analyzed materials do not seem to have a significant variation in their self-healing performance. This needs to be verified through a more accurate analysis, and the absence of intermediate irradiation steps does not allow us to determine the dose threshold at which the first self-healing performance degradation occurs. Nevertheless, this preliminary study marks the considered self-healing polymers as promising for space applications.

4 Conclusions

The presented work considers both the ability to shield human crewmembers of a supramolecular elastomer Reverlink® HR and a self-healing PUU and the effects of gamma radiation on their self-healing performance.

The first part of the study gives an estimate of the radiation equivalent doses absorbed by human tissue when directly shielded by an inflatable space habitat with either standard materials, Reverlink® HR, or self-healing PUU used to manufacture its bladder layer. The main purpose of this part is to verify that the insertion of self-healing polymers into an inflatable space system can increase its autonomy without compromising its shielding performance. In the second part, puncture tests before and after gamma irradiation by a Co60 source are also presented to look at the possible effects of radiation on the healing performance of these materials when considering an EMU case study.

According to the HZETRN2015 simulations, integrating the supramolecular elastomer bladder layer into the habitat provides the highest radiation protection. The insertion of SWCNT into this polymer is also briefly considered to determine if they can further increase its shielding performance, but as the related results show no enhancement in these terms the neat solutions are preferred to the nanocomposites since they prove to be more practical and affordable.

As concerns the self-healing performance of the materials under analysis, the puncture tests show that it does not seem to be significantly affected by the used 100 Gy dose, at least from the perspective of this initial study and of the considered EMU example. Additional analysis is nevertheless necessary to verify this outcome and to determine the threshold dose at which the self-healing performance starts to degrade.

In general, incorporating a self-healing layer into space structures like habitats for upcoming missions can considerably enhance their safety, reliability, and lifespan. However, additional research is necessary to effectively implement this solution. Furthermore, all the here-presented simulations

are performed using a slab geometry. In the future, more accurate results could be obtained through 3D numerical analysis. A complete mission should be simulated as well to analyze the equivalent dose absorbed by the self-healing and reference habitat configurations in each mission phase (e.g. transfer route, permanence on the surface of a planet or satellite). This could also lead to an initial estimate of the operational lives of the materials. Finally, additional high-velocity puncture tests will be conducted to reproduce the MMOD worst-case conditions related to chosen specific mission scenarios.

Appendix

A. Space habitat materials: data for simulations

NOTE: a common reference is considered for all the Kevlar® variants (FDI 120, KLM-705, felt), as these all possess very similar densities and are characterized by the same chemical composition.

Funding Open access funding provided by Politecnico di Milano within the CRUI-CARE Agreement. ESA Contract No. 4000132669/20/NL/MH/ic.

Declarations

Conflict of interest The authors hereby declare that they have no conflict of interest.

Material	Composition	Atoms/g (10^{22})							Density (g/cm^3)
		H	C	N	O	Al	Si	B	
Kevlar®	$C_{14}H_{12}N_2O_3$	2.81	3.29	0.47	0.705	–	–	–	1.4
Kapton®	$C_{22}H_{10}N_2O_5$	1.58	3.47	0.315	0.788	–	–	–	1.425
Mylar®	$C_{10}H_8O_4$	2.51	3.13	–	1.25	–	–	–	1.4
Nextel™	62% wt Al_2O_3 24% wt SiO_2 14% wt B_2O_3	–	–	–	1.94	0.732	0.241	0.242	2.7
PU foam	$C_{27}H_{36}N_2O_{10}$	3.95	2.97	0.22	1.10	–	–	–	0.014
Vectran®	$C_{18}H_{10}O_4$	2.08	3.74	–	0.83	–	–	–	1.4
Urethane	$NHCO_2$	1.02	1.02	1.02	2.04	–	–	–	1.13
Nylon	$C_{12}H_{24}N_2O_2$	6.33	3.16	0.527	0.527	–	–	–	1.14
Nomex®	$C_{14}H_{10}N_2O_2$	2.53	3.54	5.06	5.06	–	–	–	1.38

Nanocomposite	Atoms/g (10^{22})				Density (g/cm^3)
	H	C	N	O	
Reverlink® + 1% SWCNT	6.04	3.7	2.03	1.03	1.092
Reverlink® + 10% SWCNT	5.49	3.82	1.85	0.936	1.111

References

1. Cadogan, D., Scheir, C., Dixit, A., Ware, J., Cooper, E., Kopf, P.: Intelligent Flexible Materials for Deployable Space Structures (InFlex). In: 47th AIAA/ASME/ASCE/AHS/ASC Structures, Structural Dynamics, and Materials Conference. AIAA, Newport (2006)
2. Pernigoni, L., Grande, A.M.: Development of a supramolecular polymer based self-healing multilayer system for inflatable structures. Acta Astronaut. **177**, 697–706 (2020). https://doi.org/10.1016/j.actaastro.2020.08.025
3. Horne, R.B., Thorne, R.M., Shprits, Y.Y., Meredith, N.P., Glauert, S.A., Smith, A.J., Kanekal, S.G., Baker, D.N., Engebretson, M.J., Posch, J.L., Spasojevic, M., Inan, U.S., Pickett, J.S., Decreau, P.M.E.: Wave acceleration of electrons in the Van Allen radiation belts. Nature **437**, 227–230 (2005). https://doi.org/10.1038/nature03939
4. Lloyd, C.W., Townsend, S., Reeves, K.K.: Space Radiation. NASA (2008)
5. Duffie, J.A., Beckman, W.A.: Solar Engineering of Thermal Processes. Wiley (2013)
6. Li, X., Warden, D., Bayazitoglu, Y.: Analysis to evaluate multilayer shielding of galactic cosmic rays. J. Thermophys. Heat Transf. **32**, 525–531 (2018). https://doi.org/10.2514/1.T5292
7. Norbury, J.W., Schimmerling, W., Slaba, T.C., Azzam, E.I., Badavi, F.F., Baiocco, G., Benton, E., Bindi, V., Blakely, E.A., Blattnig, S.R., Boothman, D.A., Borak, T.B., Britten, R.A., Curtis, S., Dingfelder, M., Durante, M., Dynan, W.S., Eisch, A.J., Robin Elgart, S., Goodhead, D.T., Guida, P.M., Heilbronn, L.H., Hellweg, C.E., Huff, J.L., Kronenberg, A., La Tessa, C., Lowenstein, D.I., Miller, J., Morita, T., Narici, L., Nelson, G.A., Norman, R.B., Ottolenghi, A., Patel, Z.S., Reitz, G., Rusek, A., Schreurs, A.-S., Scott-Carnell, L.A., Semones, E., Shay, J.W., Shurshakov, V.A., Sihver, L., Simonsen, L.C., Story, M.D., Turker, M.S., Uchihori, Y., Williams, J., Zeitlin, C.J.: Galactic cosmic ray simulation at the NASA space radiation laboratory. Life Sci. Sp. Res. **8**, 38–51 (2016). https://doi.org/10.1016/j.lssr.2016.02.001
8. Waller, J.M., Rojdev, K., Shariff, K., Litteken, D.A., Hagen, R.A.: Simulated Galactic Cosmic Ray and Solar Particle Event Radiation Effects on Inflatable Habitat, Composite Habitat, Space Suit and Space Hatch Cover Materials. (2020)
9. Cohen, M.M.: Carbon Radiation Shielding for the Habot Mobile Lunar Base. Presented at the July 19 (2004)
10. Arkema: Reverlink supramolecular technology
11. Montarnal, D., Tournilhac, F., Hidalgo, M., Leibler, L.: Epoxy-based networks combining chemical and supramolecular hydrogen-bonding crosslinks. J. Polym. Sci. A Polym. Chem. **48**, 1133–1141 (2010)
12. Sordo, F., Mougnier, S.J., Loureiro, N., Tournilhac, F., Michaud, V.: Design of self-healing supramolecular rubbers with a tunable number of chemical cross-links. Macromolecules **48**, 4394–4402 (2015). https://doi.org/10.1021/acs.macromol.5b00747
13. Grande, A.M., Martin, R., Odriozola, I., van der Zwaag, S., Garcia, S.J.: Effect of the polymer structure on the viscoelastic and interfacial healing behaviour of poly(urea-urethane) networks containing aromatic disulphides. Eur. Polym. J. (2017). https://doi.org/10.1016/j.eurpolymj.2017.10.007
14. Rekondo, A., Martin, R., Ruiz de Luzuriaga, A., Cabañero, G., Grande, H.J., Odriozola, I.: Catalyst-free room-temperature self-healing elastomers based on aromatic disulfide metathesis. Mater. Horiz. **1**, 237–240 (2014). https://doi.org/10.1039/C3MH00061C
15. Cucinotta, F.A., Kim, M.-H.Y., Chappell, L.J.: Evaluating shielding approaches to reduce space radiation cancer risks. (2012)
16. Laurenzi, S., de Zanet, G., Santonicola, M.G.: Numerical investigation of radiation shielding properties of polyethylene-based nanocomposite materials in different space environments. Acta Astronaut. **170**, 530–538 (2020). https://doi.org/10.1016/j.actaastro.2020.02.027
17. NASA: HZETRN2015 User Guide, (2015)
18. Jennings, W.A.: Quantities and units in radiation protection dosimetry. Nucl. Instruments Methods Phys. Res. Sect. A Accel. Spectrometers **346**, 548–549 (1994). https://doi.org/10.1016/0168-9002(94)90590-8
19. O'Neill, P.M.: Badhwar–O'Neill galactic cosmic ray model update based on advanced composition explorer (ACE) energy spectra from 1997 to present. Adv. Sp. Res. **37**, 1727–1733 (2006). https://doi.org/10.1016/j.asr.2005.02.001
20. Badavi, F.F., West, K.J., Nealy, J.E., Wilson, J.W., Abrahms, B.L., Luetke, N.J.: A dynamic/anisotropic low Earth orbit (LEO) ionizing radiation model. Hampton (2006)
21. Singleterry, R.C.: Radiation engineering analysis of shielding materials to assess their ability to protect astronauts in deep space from energetic particle radiation. Acta Astronaut. **91**, 49–54 (2013). https://doi.org/10.1016/j.actaastro.2013.04.013